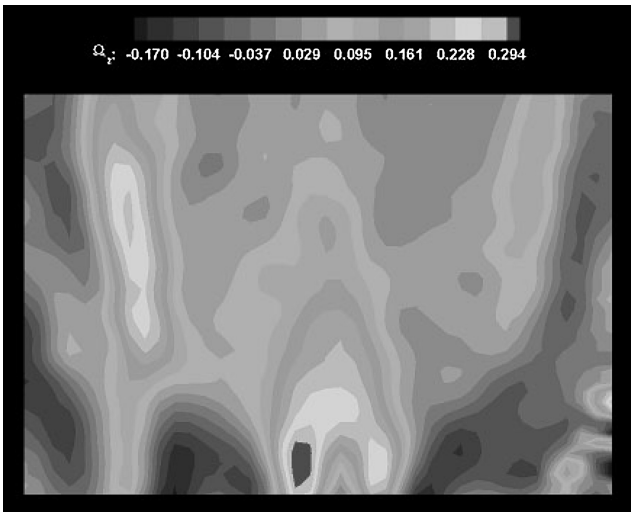

Fig. 8 Time-averaged vorticity map in the spray flame.

experimental data and predictions for the entire flow domain. The new PIV diagnostics also allow one to visualize the time resolved motion of the flow in three dimensions as a movie.

Conclusions

It has been demonstrated that the simultaneous use of mechanical shutter and narrow-bandpass interference filters can resolve overexposure problems associated with PIV diagnostics in flames, in particular luminous flames that feature high background flame radiation. The PIV system discussed here is capable of detecting fuel droplets, particles, or seed particles under a variety of flow conditions. The diagnostics allow one for the first time to obtain detailed and comprehensive information on flow dynamics associated with complex flows, including swirling flows, jets, and various kinds of practical systems under reacting and combustion conditions can be generated.

Acknowledgment

This research was supported by the Office of Naval Research with program manager Gabriel D. Roy. This support is greatly appreciated.

References

[1]Aroussi, A., Kucukgokoglan, S., Menacer, M., and Pickering, S. J., "PIV Measurements of Swirling Flows from Two Adjacent Burners," 9th International Symposium on Flow Visualization, Optical Diagnostics in Engineering, Paper 13, Aug. 2000.

[2]Nie, J. X., Yeboah, Y. D., Bota, K. B., Bai, T., and Ross, H. D., "Laser Doppler Velocimetry and Particle Image Velocimetry Measurements of Premixed Methane-Air Flames and Their Comparisons," *Proceedings of 3rd ASME/JSME Joint Fluids Engineering Conference*, ASME, New York, July 1999.

[3]Yeboah, Y. D., Nie, J. X., Bai, T., Bota, K. B., and Ross, H. D., "Particle Image Velocimetry Measurements of Premixed Methane-Air Flames," *Proceedings of 1998 American Society of Mechanical Engineers Fluids Engineering Division Summer Meeting*, ASME, New York, June 1998, pp. 1–25.

[4]Linck, M., and Gupta, A. K., "Effect of Swirl and Combustion on Flow Dynamics in Luminous Kerosene Spray Flames," AIAA 2003-1345, Jan. 2003.

[5]Habibzadeh, B., and Gupta, A. K., "Passive Control of Kerosene Spray Flame Structure in a Swirl Burner," *Proceedings of the International Conversion and Related Technologies (RAN)*, Nagoya Univ., Nagoya, Japan, Dec. 2001.

[6]Gupta, A. K., Habibzadeh, B., Archer, S., and Linck, M., "Control of Flame Structure in Spray Combustion," *Proceedings of the 15th Office of Naval Research Propulsion Meeting*, edited by G. Roy and A. K. Gupta, Univ. of Maryland, MD, Aug. 2002, pp. 29–34.

Reaction Rates for Hypergolic Propellants Using Chemical Delay Times

Mark J. Farmer,* Lynette O. Mays,*
Casey S. Hampton,* and James E. Smith Jr.†
University of Alabama In Huntsville,
Huntsville, Alabama 35899

Introduction

HYPERGOLIC bipropellants are defined as fuel and oxidizer combinations that, upon contact, chemically react and release enough heat to spontaneously ignite. Nitric acid and oxides of nitrogen are used as the oxidizer. The fuels are organic compounds including amines, heterocyclic compounds, and polyatomic phenols.

The discovery of hypergolicity occurred in Germany around 1937, and research on hypergolic bipropellant combinations spread to other countries after WWII.[1] During the 1950s, interest in hypergolic combinations grew as knowledge of their high density, high performance, and long-term storability developed. The Titan, Gemini, and Apollo programs all used hypergolic propellants. Currently the Ariane, Long March, Space Shuttle, and International Space Station programs are among the most recognizable users of hypergols.

One important measure of the hypergolic performance is the length of time between reactant contact and appearance of the flame, termed the ignition delay time (IDT). Measured in milliseconds, IDT is important because longer than desired delays can lead to lower performance or cause catastrophic failure of the engine.

This Note reports on a new laser diagnostic method to measure and examine ignition delays for hypergolic reactions. This technique, as a result of its time resolution, is the first to measure the chemical delay time (CDT) just prior to ignition. This new chemical performance measurement can be used to compare hypergolic reactions and defines the time during which free radicals generated by the reactions should be analyzed.

Equipment

The entire operating system is designed to study the reaction rates and mechanisms of hypergolic reactants for the ability to propose alternate mechanisms. The equipment uses a variety of techniques, including visible and near-infrared Raman spectroscopic measurements, to meet these objectives. The combustion chamber, supporting systems, and diagnostics have been designed and assembled as illustrated in Fig. 1. The operating system is described in detail in previous publications.[2–5]

Currently, the combustion system supports ignition and CDT studies between liquid fuel and oxidizer. Modifications can be made to study other reactive systems such as solid fuels and gelled propellants. Therefore, a wide variety of hypergolic systems can be kinetically studied in a controlled environment leading to an understanding of the mechanisms and free radicals, which control these reactions.

Received 1 September 2002; revision received 23 May 2003; accepted for publication 2 June 2003.

*Graduate Research Assistant, Department of Chemical and Materials Engineering.

†Professor, Department of Chemical and Materials Engineering. Member AIAA.

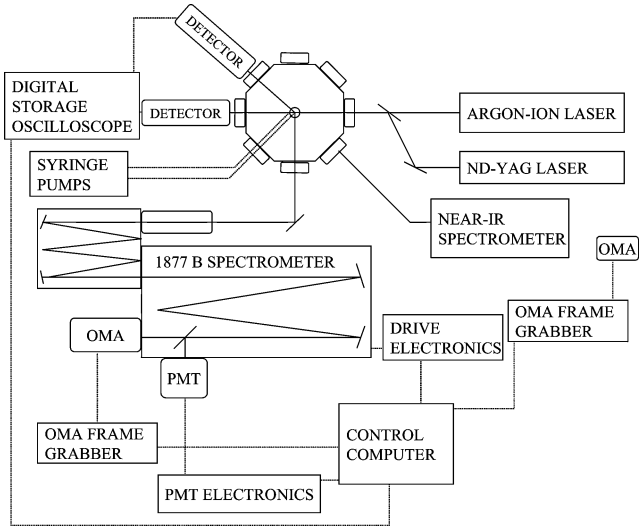

Fig. 1 Schematic of the entire CDT apparatus.

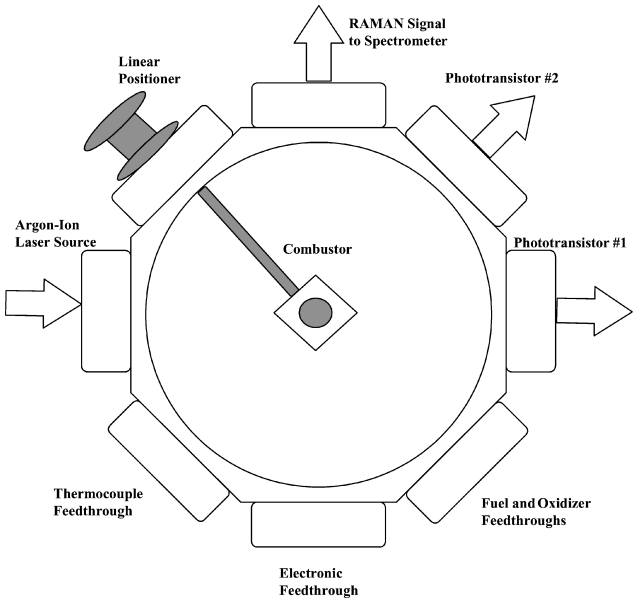

Fig. 2 Top view of the combustion chamber.

Experimental Procedure

The experimental procedures involve three main steps, namely the laser and phototransistor alignment, determining the proper oxidizer-to-fuel ratio, and measuring the response from the combustion chamber. To measure the ignition delay with the system, an argon–ion laser source is passed directly above a droplet of oxidizer within the combustor.

As shown in Fig. 2, two phototransistors are required to monitor the chamber. In operation, phototransistor #1 monitors the laser beam intensity through a pinhole 200 μm in diameter. This diode and pinhole assembly is positioned by a three-axis micropositioner. The pinhole/diode geometry restricts the view of the phototransistor to approximately 200 μm above the surface, as shown in Fig. 3.

Phototransistor #2 monitors emission from the combustor through a fixed bandpass filter that eliminates scatter from the argon–ion laser and is necessary because of the extreme sensitivity of this phototransistor throughout the visible and near-infrared spectrum. A concentrating optics are used to collect the signal. The focusing optics restrict the view of the flame by the phototransistor to a region approximately 2 mm in diameter, directly above and centered on the combustor.

Using the appropriate safety equipment under a chemical fume hood, syringes for the fuel and oxidizer are loaded with approximately 1–2 ml each. They are then taken separately to the testing area and attached to the ends of 1-m-long hypodermic needles. The laser diagnostic system is housed under an exhaust hood. A dilute sodium-hydroxide solution is nearby in case of an accidental acid spill. For a single test the amount of combined fuel and oxidizer used is generally less than 50 μl.

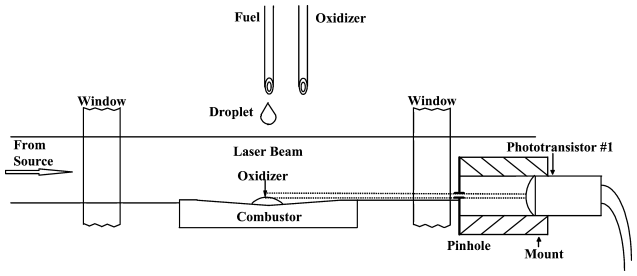

Fig. 3 Phototransistor #1 alignment.

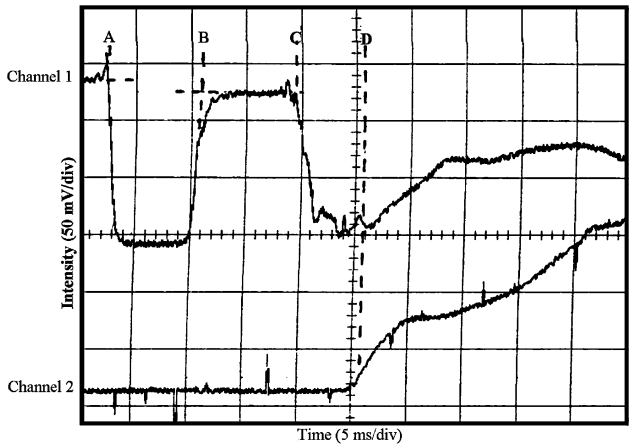

Fig. 4 Typical drop test for hydrazine/RFNA.

In operation, a measurement is made by placing a precalculated amount of oxidizer onto the combustor using a hypodermic needle as shown in Fig. 3. This calculation is based on the fuel and oxidizer droplets corresponding volume and density, and the calculation sets the desired oxidizer-to-fuel mole ratio. Once the correct oxidizer-to-fuel ratio is calculated, a fuel droplet of known volume is discharged from the hypodermic needle positioned approximately 1.5 cm above the oxidizer. This droplet passes through the laser beam and attenuates the response of phototransistor #1 and mixes with the oxidizer. At some time later a vapor phase appears and ignites with the flame sensed by phototransistor #2 and recorded on channel 2 of the oscilloscope. The time lag between these two occurrences is a direct measurement of the ignition delay time.

Test Results

Numerous tests were performed at each oxidizer-to-fuel ratio tested. The periods of droplet entry, mixing, and chemical reaction are defined within the oscilloscope traces from test results.[6,7] Finally, the importance of the chemical delay time is discussed as a reproducible measure of the chemical performance independent of the mixing technique.

Figure 4 shows the digital storage oscilloscope trace resulting from a typical drop test for hydrazine (98%) contacted with red fuming nitric acid (RFNA), 90% nitric acid the balance nitrogen tetroxide.[2] The results in this figure are for an oxidizer-to-fuel ratio of 4. Here, channel 1 shows the output from phototransistor #1, which monitors the surface of the oxidizer droplet, and channel 2 is the output from phototransistor #2, which monitors flame emission. Various reference points have been added to this figure to identify key features resulting from this technique. Point A on channel 1

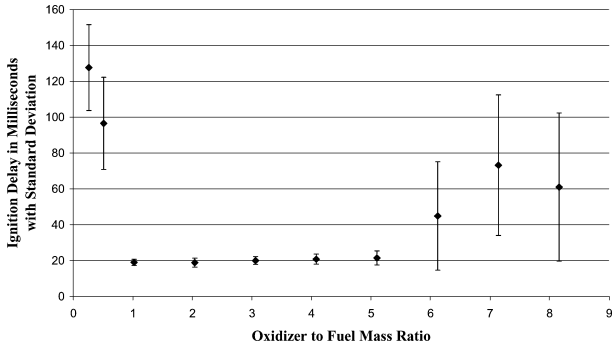

Fig. 5 Comparison of ignition delay times with varying O:F mass ratios.

represents the moment of contact between the fuel and oxidizer. The region from point A to point B represents the droplet of fuel from initial contact to final entry into the oxidizer. The response of phototransistor #1 in the region from point B to C is representative of a still liquid-to-air interface. At point C the chemical reaction rate increases rapidly, with the reaction producing a vapor phase. This vapor phase was noticed in the work of Ladanyi and Miller using an injector technique with high-speed photography.[8] The combination of heat release from the chemical reaction in the liquid phase and the reactivity of the gaseous intermediates causes ignition in the vapor phase, as defined by point D. The analysis presented is also supported by others.[9–12]

Kilpatrick and Baker stated, "If the complete intermixing could be effected in a time very short compared to the (total) ignition delay time, then the measured delay would be the true chemical delay . . ."[13] Therefore, if the droplet entry and mixing stages, points A–C, could be eliminated or measured as accomplished here, then region C–D in Fig. 4 would represent the true chemical delay devoid of mixing.

Another phenomenon observed between points C and D is the rapid fluctuation of the signal from phototransistor #1. Paushkin observed vigorous boiling in the liquid mixture prior to ignition of the vapor.[14] Broatch obtained results using high-speed photography showing boiling in the liquid phase prior to vapor ignition for both a drop tester and impinging jets.[15] The fluctuation of channel 1 between C and D is likely the result of this vigorous boiling.

Bias error for the laser diagnostic technique originates from the oscilloscope traces. The bias error for the hydrazine test results was ± 1 ms. For the unsymetric dimethyl-hydrazine (UDMH) test results shown later, the bias error was ± 0.4 ms. Test results from hydrazine/RFNA using the classic definition for ignition delay time, region A–D in Fig. 4, are shown in Fig. 5 for varying oxidizer-to-fuel ratios. Figure 5 represents over 100 tests with 10 tests at each oxidizer-to-fuel ratio.[2] Standard deviation was chosen to represent the precision error.

Fuel-rich or oxidizer ratios became very unpredictable, as shown by the standard deviations. Pino noted that either the ignition delay was significantly longer or a popping (explosive) type result occurred when he had less than adequate mixing.[16] For a test with poor mixing, the interface between the fuel and oxidizer has regions of extremely high- and low-oxidizer concentrations. The popping phenomenon was noted at high oxidizer-to-fuel ratios. This would be similar to a poor mixing condition causing the same extreme oxidizer-to-fuel ratios. A response of this type is shown in Fig. 6 for an oxidizer-to-fuel mole ratio of 12 for hydrazine and RFNA. Region A–C in Fig. 6 is similar to the other test, but after point C a high-frequency repulsion of the reactants occurs resulting in popping but no flame.

At the other extreme are the high fuel ratios where extremely long ignition delays occur because of the limited amount of oxidizer to support the reaction. The chemistry of the extreme oxidizer-to-fuel ratios would be an area of useful information during the spectroscopic analysis of these reactions and should be examined along with optimum ratios.

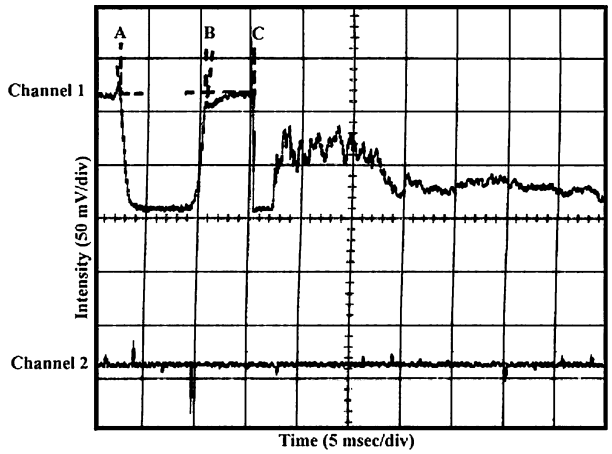

Fig. 6 Typical drop test when popping occurred.

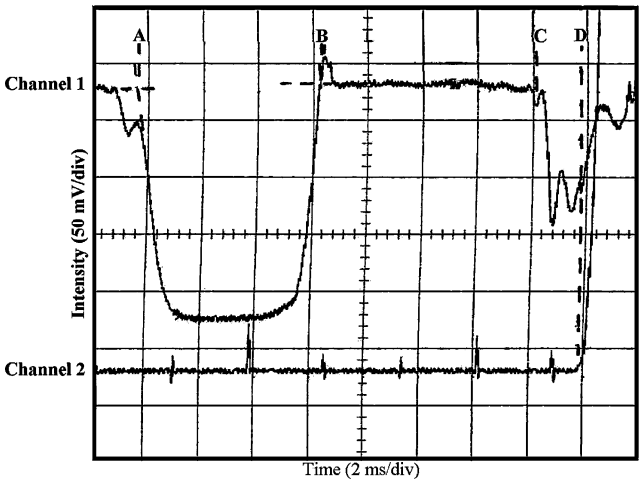

Fig. 7 Typical drop test for UDMH/RFNA.

The IDT values for the hydrazine/RFNA system shown in Fig. 5 are a function of the testing technique and therefore no more valuable than previous drop-test results. In other words, these numbers can only describe relative performance of different fuels and oxidizers and can in no way predict the performance in a specific engine. However, if we reexamine these tests from point C to D, as shown in Fig. 4, then we are measuring chemical performance. This chemical delay time is characteristic of chemical composition, temperature, and pressure, thus the chemical reactions taking place. The performance from point C to D is not dependent upon the method of mixing. This region from point C to D represents the first measure of chemical performance for hypergolic combustion.

Figure 7 is a typical test result for UDMH/RFNA at the same composition as the hydrazine tests and an oxidizer-to-fuel ratio of 3.8. The total ignition delay for this test was 16.5 ms. Region C-D was significantly shorter for UDMH than hydrazine, suggesting a more vigorous reaction. To illustrate this point, Table 1 shows the calculated chemical and ignition delay times for these two hypergols. If one compares the average ignition delay of UDMH to hydrazine for set oxidizer-to-fuel ratios, the ignition delay of UDMH is 14 ± 2 ms, and 19 ± 2 ms for hydrazine. The ignition delay of UDMH has a 25% decrease compared to hydrazine. However, if the average chemical delay times are examined, region C-D, the chemical delay of UDMH is 2.0 ± 0.5 ms, whereas the chemical delay of hydrazine is 7.5 ± 1.0 ms. The chemical delay time of UDMH has a 75% decrease in magnitude from the chemical delay time of hydrazine. In other words, UDMH/RFNA reacts approximately four times faster than hydrazine/RFNA.

The strength of the response in channel 2 at point D reflects the weaker reactivity of hydrazine. The slopes were averaged for set

Table 1 Ignition and chemical delay times for hydrazine and UDMH

RFNA/Hydrazine			RFNA/UDMH		
O:F mass ratio	Ignition delay time, ms	Chemical delay time, ms	O:F mass ratio	Ignition delay time, ms	Chemical delay time, ms
1.02	18	8.0	4.08	16	2.0
1.02	19	8.0	4.08	14	1.5
1.02	18	7.5	4.08	14	2.0
1.02	20	6.0	4.08	14	2.5
1.02	20	8.0	4.08	13	2.5
1.02	16	6.0	4.08	15	2.0
1.02	21	8.0	4.08	11	2.0
1.02	19	9.0	4.08	14	3.0
1.02	16	5.5	4.08	17	Unclear
1.02	17	8.0	4.08	14	Unclear
1.02	21	8.0	——	——	——
1.02	17	8.0	——	——	——
1.02	21	Unclear	——	——	——
1.02	21	Unclear	——	——	——
1.02	18	Unclear	——	——	——
1.02	21	Unclear	——	——	——
Average	19	7.5	Average	14	2.0
Standard deviation	2.0	1.0	Standard deviation	2.0	0.5

Table 2 Relative comparison of ignition response

O:F mass ratio	Initial slope, mV/ms	O:F mass ratio	Initial slopes, mV/ms
2.04	25	4.08	200
2.04	25	4.08	200
2.04	19	4.08	267
2.04	19	4.08	400
2.04	50	4.08	400
2.04	38	4.08	175
2.04	13	4.08	400
2.04	13	4.08	400
2.04	10	4.08	200
2.04	13	4.08	400
2.04	8	——	——
2.04	13	——	——
2.04	19	——	——
2.04	32	——	——
Average	21	Average	304
Standard deviation	12	Standard deviation	104

oxidizer-to-fuel ratios with the calculations presented in Table 2. The slope of channel 2 for hydrazine was 20 ± 12 mV/ms. The slope of channel 2 for UDMH was approximately 15 times that of hydrazine at 300 ± 100 mV/ms. The slope of the output signal of channel 2 is related to both the gas generation from the liquid phase and reaction kinetics in the vapor phase. The thick vapor phase makes the standard deviation of these results large, but the difference is response is still quite clear.

Conclusions

Regardless of technique, mixing is a limitation of any system. Spengler and Bauer noted that the ignition delay determined by any system is valid only for that system and should never be used as a performance parameter for a rocket engine unless the ignition delay times were recorded with that specific rocket engine.[9] The technique presented here can accurately and with reproducibility measure ignition delay times. In addition, the direct measurement of region C-D provides chemical delay times, a more true comparison of chemical kinetics.

As fuels and oxidizers must be mixed, a time delay for mixing is unavoidable. Droplets must be large enough to support combustion, which further increases mixing time. The results and discussions of this new technique revealed a region after mixing that characterizes the speed of the chemical reactions. This region represents the first measure of chemical performance independent of mixing technique. This CDT is a function of chemical composition, temperature, and pressure, thus the chemical reactions taking place. The CDT was shown to be a very reproducible measurement at certain oxidizer-to-fuel ratios for the two fuels tested. The CDT can be used to quantify accurately the reactant performance of current hypergolic systems and any future combinations tested in this research. In summary, a safe, cost-effective, diagnostic method to measure ignition delays has been shown to provide important information on the chemical reactions through the CDT.

Acknowledgments

This material is based upon work supported by, or in part by, the U.S. Army Missile Command, under Grant Number DAA H01-91-D R002/D053, also, the U.S. Army Research Laboratory and the U. S. Army Research Office under Grant Numbers DAAD190210356 and DAA H04-94-G-0265. The authors also wish to thank the support of the University of Alabama in Huntsville's Propulsion and Optics Research Centers.

References

[1]Zarchan, P., *Liquid Rocket Engine Combustion Instability*, Vol. 169, AIAA, Washington, DC, 1995, pp. 113–142.

[2]Farmer, M. J., "A Study of the Reaction Rates of Hypergolic Propellants," M.S. Thesis, Dept. of Chemical and Material Engineering, Univ. of Alabama in Huntsville, May 1997.

[3]Mays, L. O., "Analysis of Chemical Delay Time in Hypergolic Fuel and Fuel Mixtures," M.S. Thesis, Dept. of Chemical and Material Engineering, Univ. of Alabama in Huntsville, Sept. 1998.

[4]Mays, L. O., Farmer, M. J., Smith, J. E., Jr., "A Laser Diagnostic Technique to Measure Chemical Delay Time in Hypergolic Combustion," *Combustion Science and Technology*, Vol. 134, 1998, pp. 127–138.

[5]Hampton, C. S., Ramesh, K. K., Smith, J. E., Jr., "Importance of Chemical Delay Time in Understanding Hypergolic Ignition Behaviors," AIAA Paper 2003-1359, AIAA 41st Aerospace Science Meeting and Exhibit, Reno, NV, Jan. 2003.

[6]Farmer, M. J., Mays, L. O., and Smith, J. E., "A Laser Diagnostic Method to Measure Ignition Time Delays of Hypergolic Reactions," AIAA Paper 97, Jan. 1997.

[7]Farmer, M. J., Mays, L. O., and Smith, J. E., "A Laser Diagnostic Technique to Measure Rapid Acid-Organic Reaction Phenomena," AICHE Paper 140e, AICHE Annual Spring Meeting, Houston, TX, March 1997.

[8]Ladanyi, D. J., and Miller, R. O., "Two Methods for Measuring Ignition Delay of Self Igniting Rocket Propellant Combinations," *Jet Propulsion*, Vol. 26, No. 3, 1956, pp. 157–63.

[9]Schmidt, E. W., *Hydrazines and Its Derivatives*, Vols. 1 and 2, Wiley-Interscience, New York, 2001.

[10]Saad, M. A., and Goldwasser, S. R., "Role of Pressure in Spontaneous Ignition," *AIAA Journal*, Vol. 7, No. 8, 1969, pp. 1574–1581.

[11]Twardy, H., "Studies on the Effect of Fuel Injection on the Ignition Process of the Hydrazine-Nitric Acid System," Jet Propulsion Lab., DLR FB 68-85, Pasadena, CA, June 1969.
[12]Habiballah, M., Dubois, I., Gicquel, P., and Foucaud, R., "Experimental Study of Combustion Processes Involved in Hypergolic Propellant Coaxial Injector Operation," AIAA Paper 92-3388, July 1992.
[13]Kilpatrick, M., and Baker, L., *Fifth Symposium on Combustion*, The Combustion Institute, New York-London, 1955, pp. 170–196.
[14]Paushkin, Y. M., *The Chemical Composition and Properties of Fuels for Jet Propulsion*, Pergamon, New York, 1962, p. 327.
[15]Broatch, J. D., "An Apparatus for the Measurement of Ignition Delays of Self-Igniting Fuels," *Fuels*, Vol. 29, 1950, pp. 106–109.
[16]Pino, M. A., "A Versatile Ignition Delay Tester for Self-Igniting Rocket Propellants," *Jet Propulsion*, Vol 25, No. 9, 1955, pp. 463–466.

Propulsion System Instability for Concentric Tank-Type Launch Vehicle

Olexiy Nikolayev*
Institute of Engineering Mechanics, Dniepropetrovsk 49005, Ukraine
and
Keiji Komatsu†
National Aerospace Laboratory, Tokyo 181-0015, Japan

Nomenclature

E = Young's modulus elasticity of tank wall material
F = area of a pipeline cross section
G = weight flow rate of fluid
g = free-fall acceleration
H = height of fluid in a tank
h = wall thickness
$\bar{N}_z$ = longitudinal load factor of a launch vehicle
n = rotation speed of a turbopump shaft
p = pressure of fluid
R = radius of tank
s = variable in the Laplace transform
V_c = cavity volume
Z = impedance of a hydraulic line
ρ = fluid density

Subscripts

1 = pump inlet
2 = pump outlet
e = external (oxidizer) tank
i = internal (fuel) tank

Introduction

THERE have been many ideas for reusable launch vehicles[1] that are recognized for their successful state-of-the-art design, but further weight reduction and improvement of specific impulse must be achieved for the next generation of reusable launch vehicles. For structural weight reduction, concentric tank configuration[2] is a possible design concept. At present, due to recent advances in polymer membrane/film materials, the possibility of the design of an inner membrane tank[3] exists. Because of the geometrical arrangement (the shortness of the feedlines, etc.) and flexibility of the inner tank, propulsion system stability margins may be changed in comparison with those of the conventional tandem tank configuration. In this Note, the propulsion system stability of the concentric tank configuration is investigated.

Linear Dynamic System Modeling

Instability caused by the cavitation phenomenon in rocket inducer-type pumps[4–6] is one type of propulsion system instability. Liquid oscillations may be revealed in a frequency range of up to 100 Hz. The stability condition for a single hydraulic line of the propulsion system on the frequency, specified by the equation

$$\operatorname{Im} Z_{\text{sys}}(s) = 0$$

can be written as follows:

$$\operatorname{Re} Z_{\text{sys}}(s) > 0 \tag{1}$$

where $Z_{\text{sys}}(s)$ is the system hydraulic impedance that is the ratio of the amplitude of pressure oscillation to the amplitude of weight flow rate oscillation, given by $Z_{\text{sys}}(s) = Z_{\text{fl}}(s) + Z_{\text{eng}}(s)$, where $Z_{\text{fl}}(s)$ is the feed system input impedance if the feed system output impedance is equal zero and $Z_{\text{eng}}(s)$ is the input impedance of the engine. The real part of input impedance of a rocket engine can be negative in some frequency ranges.[5] For the small hydraulic resistance of engine feed lines, self-excited oscillations are quite possible for such a propulsion system.

Propulsion system dynamics can be described by a set of the differential equations in the lumped and distributed parameters. The parameters of the system are determined by geometrical and mechanical properties of the propulsion system of the launch vehicle. The key point for the modeling dynamics of the propulsion system is the accurate description of the dynamic properties of cavitating pumps. In accordance with a hydrodynamic unsteady-state mathematical model,[4,5] cavitating inducer-type centrifugal pump dynamics is described by the following equations[4]:

$$\delta p_1 = (B_1 + B_1 T_c s)\delta V_c + (B_2 + L_{\text{ind}} s)\delta G_1 + (A + Ds)\,\delta n \tag{2}$$

$$\rho g\, s\delta V_c = \delta G_2 - \delta G_1 \tag{3}$$

$$\delta p_2 = \delta p_1 + (s_p - L_p s)\delta G_2 + \varepsilon \delta V_c + T_n \delta n \tag{4}$$

where s_p is the partial derivative to the dependence of the pump head rise on the volume of cavities, ε is the partial derivative to the dependence of the pump head rise on fluid weight flow rate, L_p is the coefficient of the pressure inertial losses in pump flow passages, B_1 is the cavity elasticity, B_2 is the negative cavitation resistance at the inducer-type pump inlet, T_c is the cavity time constant,[4] L_{ind} is the coefficient of the pressure inertial loss in inducer vane passages on the section of the cavity height growth,[4] A and D are the rotational coefficients, and T_n is the partial derivative to the dependence of the pump head rise on the pump shaft rotation speed. Here and subsequently, δ is used for the parameter perturbation.

The dynamic behaviors of feedlines and of oxidizer and fuel tanks are modeled by assembling the tandem pipeline elements. Each element is described by the equations of the unsteady one-dimensional motion of a compressible fluid in the distributed parameters. The equations connect the parameters of the unsteady motion of fluid (pressures and weight flow rates) at the initial, $x = 0$, and any, $x > 0$, cross section of the element considered. They are given by

$$\delta p(x,\ s) = \delta p(0,\ s)\cosh\gamma(s)x - \delta G(0, s) Z_w(s)\sinh\gamma(s)x$$

$$\delta G(x, s) = -\frac{\delta p(0, s)}{Z_w(s)}\sinh\gamma(s)x + \delta G(0, s)\cosh\gamma(s)x \tag{5}$$

where $\gamma(s) = \sqrt{[Z_1(s)Y_1(s)]}$ is the complex constant of wave propagation per unit of length of the pipeline element, $Z_w(s) = \sqrt{[Z_1(s)/Y_1(s)]}$ is the wave resistance of the pipeline element,

Received 7 July 2002; revision received 12 May 2003; accepted for publication 7 July 2003.

*Senior Scientific Researcher, Structural and Hydraulic Division.
†Senior Staff Researcher, Structures and Materials Research Center, Osawa 6-13-1. Member AIAA.